GSOE Wind

Turbine Design

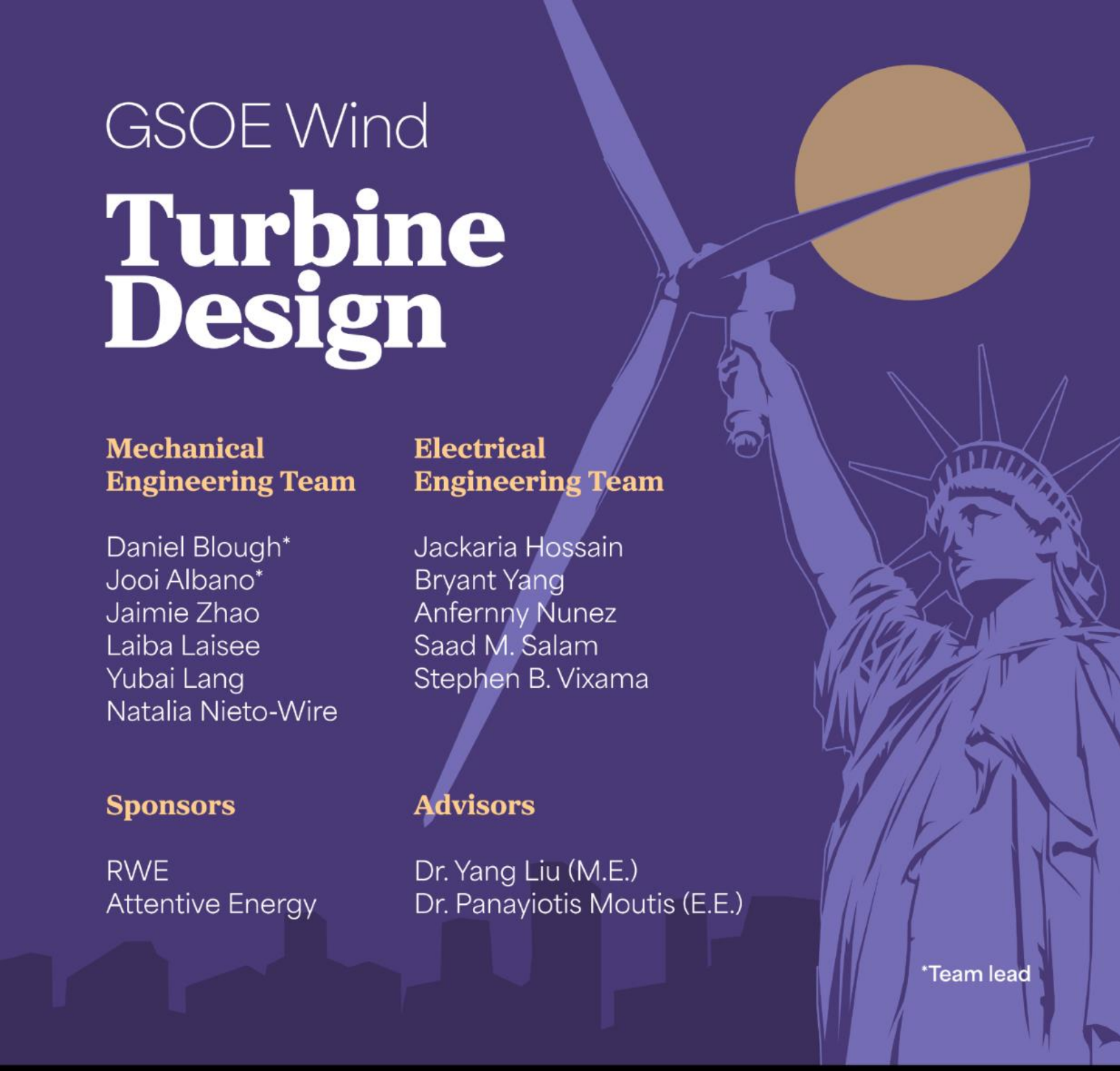

Mechanical Engineering Team

Daniel Blough*
Jooi Albano*
Jaimie Zhao
Laiba Laisee
Yubai Lang
Natalia Nieto-Wire

Electrical Engineering Team

Jackaria Hossain
Bryant Yang
Anfernny Nunez
Saad M. Salam
Stephen B. Vixama

Sponsors

RWE
Attentive Energy

Advisors

Dr. Yang Liu (M.E.)
Dr. Panayiotis Moutis (E.E.)

*Team lead

www.gsoewind.com | gsoe.cwc2024@gmail.com | (845) 240-5396

GSOE WIND

RWE attentive energy

The City College of New York
The Grove School of Engineering
275 Convent Avenue, New York, NY 10031

Contents

Figure 1: Turbine solidworks (left) Turbine Prototype (right)

Executive Summary

As a first-year team, GSOE (Grove School of Engineering) Wind at the City College of New York set about developing an off-shore wind turbine that meets the requirements set in place by the Collegiate Wind Competition. The aim was to maximize efficiency and reliability.

To accomplish this, we selected an MH112 airfoil using QBlade for the optimization process. Optimization consisted of thorough analysis of the Schmitz limit for angle of twist and the Blade Momentum Theory. Optimization measures were taken to lower the Reynolds number, and blades were printed using carbon fiber PLA. Final blade composition was determined by testing various printable materials including PLA, resin and carbon fiber PLA. The final choice of CF PLA was based on optimizing stiffness, weight, and surface quality.

Significant resources were put towards developing a versatile but simple pitching system as pitching was determined to contribute to a large amount of scoring. After many iterations, we arrived at a rack and spur gear system that when tested, proved versatile but simple to manufacture and iterate.

A streamline nacelle and nosecone were developed to minimize force on the foundation and the foundation was optimized for weight vs strength. To do so, we arrived at a barbed bucket design out of 20-gauge mild steel to harness the tensile strength needed on the front end of the foundation and compression on the back. Strategic bends give our foundation necessary rigidity, and helical piles and barbs secure it to the sand pit.

The turbine and load electronic components are housed within two separate NEMA 1 electrical enclosures. Ventilation holes, heat sinks, and a computer fan were all implemented to ensure proper heat rejection. Two Arduino microcontrollers were incorporated in our design for communication and control of our in-house 24V boost converter, electronic load, and turbine electronic devices. Both microcontrollers are housed in the load enclosure. The turbine side of the PCC incorporates a 24V generator and 24V boost converter. The total capacitive energy storage within the turbine side was calculated to 2.6J which is well within the competition requirement of 10J maximum. The load side of the PCC contains a current sink electronic load utilizing MOSFETs and operational amplifiers.

Design Objectives

GSOE Wind aims to design a fixed-bottom offshore wind turbine that can withstand winds up to 22 m/s, that starts to generate power at 5 m/s and has stable rated power output in the 11 m/s – 14m/s wind speed range with an emergency capacity. To achieve these objectives, our team divided the turbine into major components and identified initial design goals for each. For blades, the goal was to design a blade with a swept area under 0.158 m^2 and capable of producing maximum power at 5-11 m/s wind speed. For pitching, the goal was to design a system capable of delivering at least 120 degrees of rotational movement. For the nacelle, an aerodynamically favorable shape while providing adequate support for all the components housed in the nacelle, while remaining withing the space allotted space. The yaw was set to be passive allowing for alignment after assembly and withstand the torque on the nacelle during durability testing. Similarly, for the tower the goal was to be able to support the weight and the wind load, while remaining within size specifications. Also, the tower was to have adequate height adjustment to align with the air flow center during commissioning. The foundation must be made entirely of ferrous material and be as light as possible while maintaining structural integrity during testing. The foundation must remain within the specified size and be installed with only tools contacting the water. Finally, control systems and electrical components will be designed to maximize the power

produced and efficiency while ensuring the turbine runs smoothly and shuts down during emergencies.

Insights From Previous Teams

As a first-year participant in the CWC, our team referenced the design reports of other teams to initiate the design process. We reviewed reports from recent years and focused on significant trends to determine the most effective design and identify the type of testing needed to ensure good turbine performance and safety. Additionally, the resources provided by the DOE and NREL were very helpful during the initial stages, enabling us to prioritize tasks effectively.

First, we decided to build a horizontal axis turbine (HAWT) with 3 blades. Considering the range of wind speed, and the special flow condition of the wind tunnel, we first assumed the most effective design is HAWT with 3 blades and confirmed it via review of past team reports. To design the drivetrain, we considered adding a gearbox initially to increase rotations per minute (RPM) but abandoned that idea after reviewing reports. Based on the other team's performance, we decided that we do not need the additional mechanical loss. Also, we chose to use a brushless direct current (BLDC) motor as a generator and got a range of possible candidates through reviewing and researching. The importance of a dynamometer was also a key insight gained from resource reviewing; we were able to set up multiple testing with dynamometer, most importantly the performance of BLDC motors as generators. Finally, for controlling the turbine, we decided to use a look up table with control input from a wind sensor, after considering maximum point tracking. As mentioned in other team reports, using MPPT will be energetically less favorable and since the turbine will operate in a wind tunnel with minimal fluctuation look up table will be the most efficient way to ensure our turbine generates maximum power.

Design

Blades

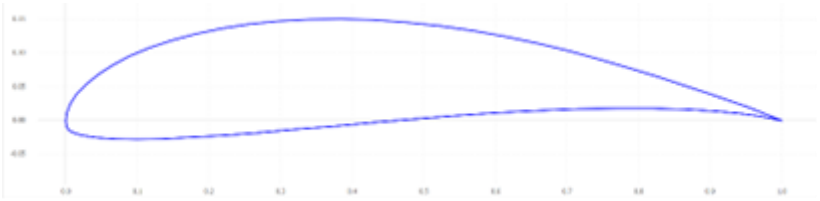

Figure 2:Airfoil profile of MH 112

To find the most suitable airfoil for our turbine, we first approximated the Reynolds number at around 80,000. MH 38 was selected as our initial airfoil as it has a high C_L and good stall behavior, but after printing it and performing a static bending test it was evident that the blade will not be able to stably operate in higher wind speeds (>15 m/s), so we decided to go for a thicker airfoil, and tested NACA 2408, NACA 2412 and MH 112. Through QBlade simulations and wind tunnel testing it was determined that MH 112 would produce higher RPMs and thus have higher C_P.

To maximize C_P of MH 112, first we found the optimal TSR was 4 (we considered balance between cut in and rated speed performance) for our applications. Next, the blade length was decided to be around 18 cm, to be within the size limit with the hub radius of 3.5cm. The chord length and angle of twist were optimized using Schmitz limit and the blade element momentum theory on QBlade. The blade was 3D printed using chopped carbon fiber PLA, with 20% infill to have structural integrity while still being light (30.416 g).

We tested the performance of the blade in the wind tunnel with no electrical loads attached to confirm RPM predictions from Qblade. Unfortunately, the maximum windspeed our wind tunnel can go up to is 10.0 m/s, so we were only able to check the RPM until 10.0 m/s. As seen by fig.4, the test results are

in good agreement with data from Qblade, thus we can confidently state that the RPM at 11 m/s will be around 2170.

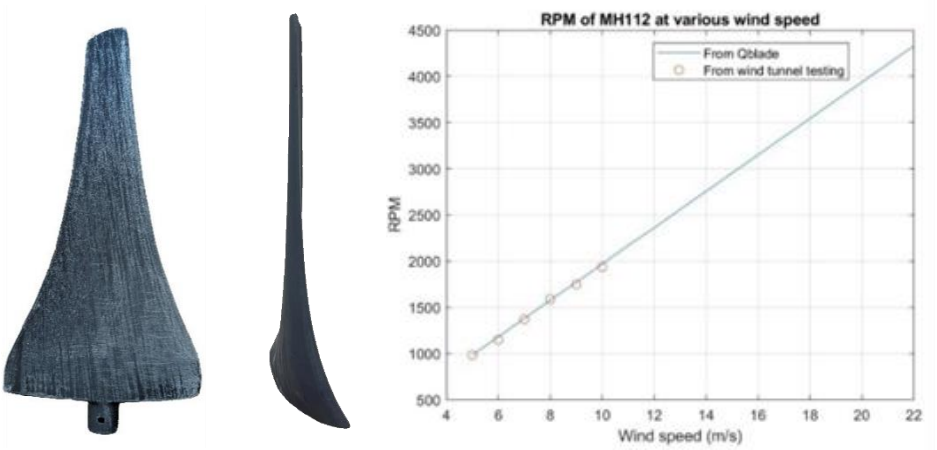

Figure 3:RPM test results vs RPM prediction from Qblade (right) and final blade printed, side view and frontal view (left)

Load Testing

Figure 4: deflection test

To test the stiffness of the 3D printed blade, we clamped the base of the blade into a vice and pushed the tip of the blade with a force gauge until it broke. The maximum force recorded was 25.02 N with corresponding deflection of 38.1 mm. We are expecting 30N of total thrust force at 22 m/s, so for one blade it will be 10 N. In conclusion, our blade has safety factor of 2.5, and if we assume the deflection to be linear at 10 N the tip deflection will be 15.22 mm, which means our blade will not hit the tower or nacelle at the maximum loading condition.

Pitching

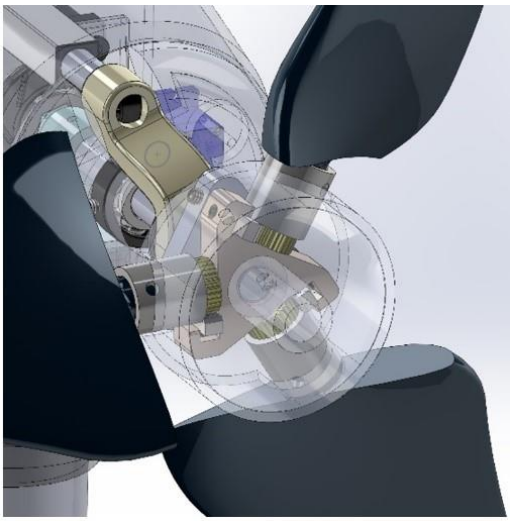

Figure 5: hub assembly

For our pitching system, we implemented a rigorous iterative design cycle with functionality, simplicity, and manufacturability as our focus. Stepping away from the traditional swashplate and push-arm system, we developed a rack and spur gear mechanism. While early iterations consisted of 6061 aluminum parts, that method proved to be limited by CNC capabilities and time consuming. Transitioning to carbon fiber 3D prints, we were able to develop a simple, effective, and versatile design, accomplishing 120 degrees of rotation with only 0.5 inches of swashplate travel. Mod 0.5 spur and rack gears made of hardened steel were chosen to achieve this. To allow for secure fastening but ease of blade rotation, the blade mounts were secured using shoulder bolts. An Actuonix L-16R was selected for facilitating pitching angle because of its significant back drive force (ability to hold in place while no power is supplied) and

Arduino controllability. The back drive force of the actuator is 102 N [1], the maximum thrust on the blades is around 30 N, giving out actuator safety factor of 3.4. To achieve linear motion in phase with the rotor, we implemented a keyed shaft that engages with the push plate. The linear actuator was extended to reach the swashplate and a combination of thrust and roller bearings (rated at 13,000rpms) were used to minimize resistance. Finally, to achieve maximum gear engagement and minimize binding, a series of set screws were used to provide adjustability to the gear alignment.

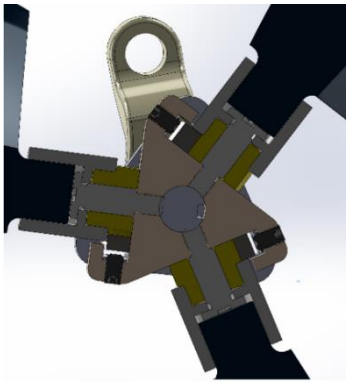

Figure 6: pitching cross section.

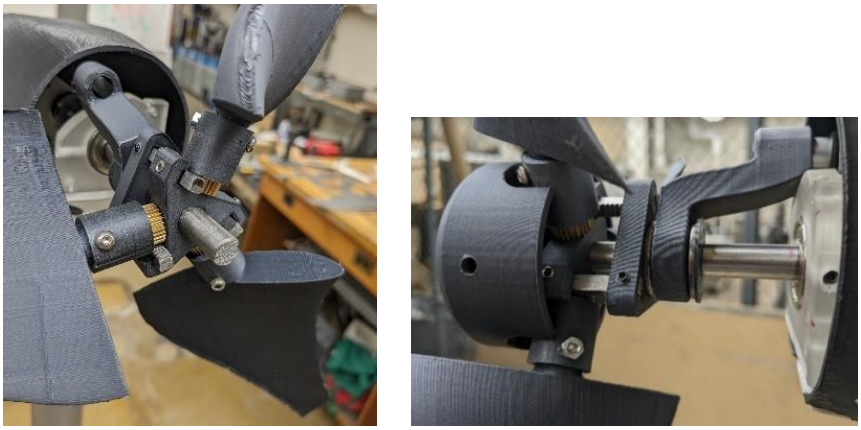

Figure 7:The nose cone mounted on the shaft (right), the picture of hub without the cone (left)

As seen in figure 7, a nose cone was printed to increase aerodynamicity of our turbine, which is secured to the drive shaft using a set screw.

For the rotor hub and pitching system, we ran finite element analysis (FEM) on the base of our blade and on the bolt that connects the base of the blade to the hub center. The centrifugal force was calculated with $F_c = m\omega^2 r$ where m is the mass of the blade, ω is the rotational speed of the blade and r is the distance from the center of rotation to the centroid. If we assume our braking does not fail, the maximum centrifugal force will be 72 N, and if we fail to control the RPM it will be 288 N

Using this freewheel centripetal force for the FEM, the stress does not exceed that of what carbon fiber PLA is rated for (43.83MPA) and displacement is minimal as shown in Figure (8).

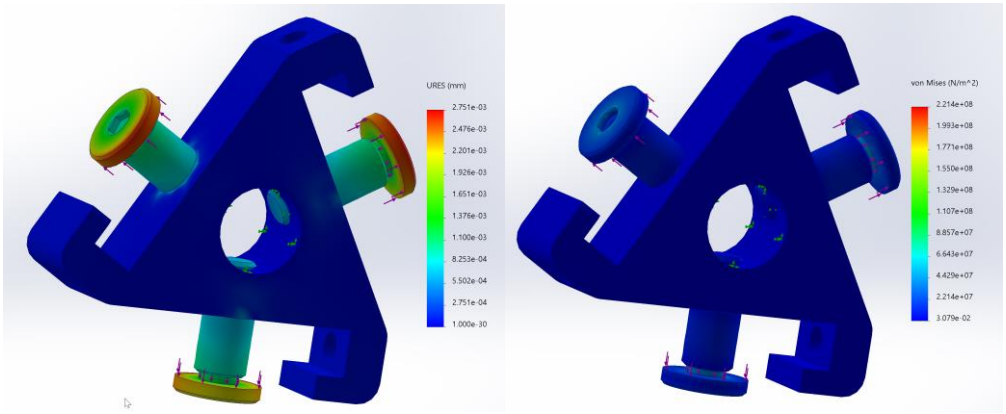

Figure 8: displacement (left) von Mises stress (right

Nacelle, Yaw, Tower

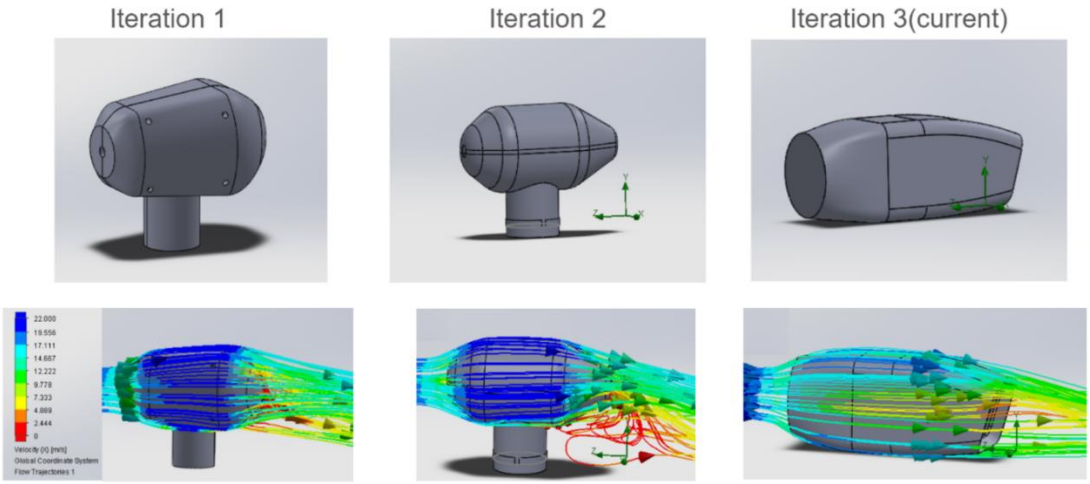

Figure 9:Design of each iteration (above three) and corresponding CFD results (below three, they all share same scale).

Iteration	1	2	3
Radius(m)	0.065887135	0.05	0.041275
Length(m)	0.2	0.2	0.2032
Cd	1.0	0.85	0.81
Drag Force(N)	4.0430	1.9791	1.3486

Table 1. The specifications and drag force of each nacelle iteration.

The nacelle was designed to minimize drag

$$D = \frac{1}{2}\rho A U^2 C_d$$

(where ρ is the density of air, A is the cross-sectional area of the structure, U is the speed of the wind and C_d is the drag coefficient) which was calculated for each nacelle design iteration. After running simulations on SolidWorks Flow Simulation, we decided to adopt the 3rd iteration as our nacelle design as it has the lowest drag, 1.349 N. The tower is 1/8-inch-thick aluminum 6061 tube with inner diameter of 1.5 inches, to ensure the wires and connections can pass through while still being able to hold the load. Using the same drag equation, the drag on tower was found to be 8.697 N.

Figure 10:xray view of pasive yaw (left) yaw force testing (right)

We chose to use a lockable yaw for our required passive yaw system. The nacelle will fit over a sleeve bearing that is held on the tower with a snap ring. The nacelle will be able to rotate around the tower and once oriented in the direction facing the incoming wind, we can clamp the nacelle and rotor components in place using bolts that squeeze the bottom sleeve of the nacelle to the

tower. Isolated yaw testing was done by applying a force up to 25.01 N to the nacelle at 6in from the tower center, which validated that the clamp force can withstand the expected yaw moment (1.85 N·m) on the turbine with a safety factor of 1.89.

Foundation

Figure 12: final foundation

For the foundation, the design parameters included size constraints (30x30x20cm with a 1.5inOD stem), weight optimization, mechanical holding force and installation with only tools touching the water. This was to be accomplished without violating the no excavation policy. Early prototyping included helical anchor, round bucket, and square bucket designs. Finding significantly more holding force in the helical anchor and square bucket, we set about identifying the physics properties responsible for these findings. Narrowing in on the way the bucket harness the compressibility of the sand and the anchor harnesses the weight of the column of sand above it, we set about maximizing the effectiveness of these two principles. After further analysis, we identified the front of the foundation was under tension and the back was under compression. After many iterations, we arrived at a design that implements two helical anchors in tension at the front of the bucket and a platform continuation at the back to harness the compression. Initially manufactured out of 16-gauge stainless steel, the square bucket proved difficult to insert into the sand. Ease of insertion was achieve by decreasing the depth of the bucket and eliminating surface area that did not contribute to the holding force. While this decreased the weight significantly, further optimization was achieved by switching to mild steel (lighter for its size) and decreasing the thickness to 20-gauge, adding strategic bends and rips so as to maintain structural integrity. To further improve holding force, barbs were added to the front end of the turbine. These helped with the structural integrity as well. Finally, a stem was attached to competition specs. The mention structure components were assembled using a combination of MIG, TIG and spot welding inhouse.

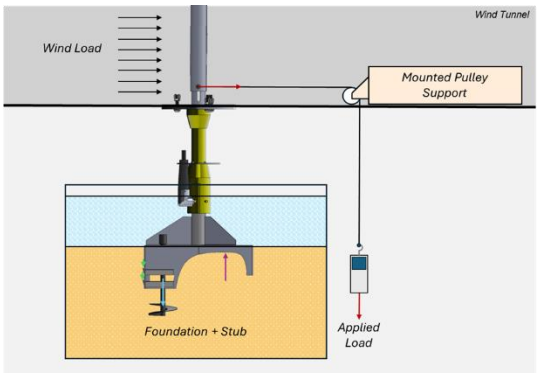

Figure 11:lateral load testing

To confirm our final design exceeded predicted and experimental thrust force, lateral load testing was performed as shown in figure (12). Experimental testing of the turbines thrust matched theoretical produced by QBlade up to 10m/s (our tunnels max) and theoretical thrust at 22m/s if the breaks fail is 30N at 90cm from the foundation. This produces a torque of 27Nm of torque. Experimental lateral load testing of the foundation resulted in maxing our force sensor out at 48.32N at 86cm from the foundation. The resulting torque was 41.55Nm. This gives our foundation a safety factor of 1.54.

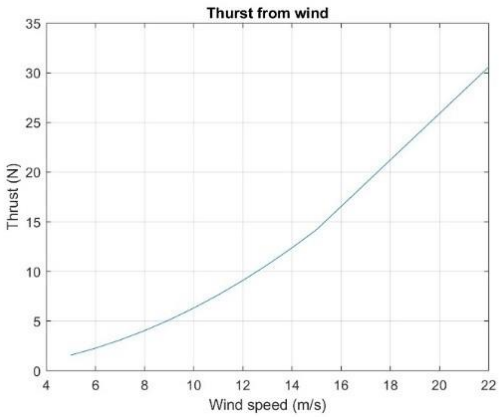

Figure 13: theoretical thrust.

GENERATOR SELECTION:

A dynamometer was designed and built in-house to test the efficiency of our generator pre-selections. A Flipsky BLDC Belt Motor 6354 was coupled to an FSESC6.7 speed controller to provide the prime mover power that would spin our test generators.

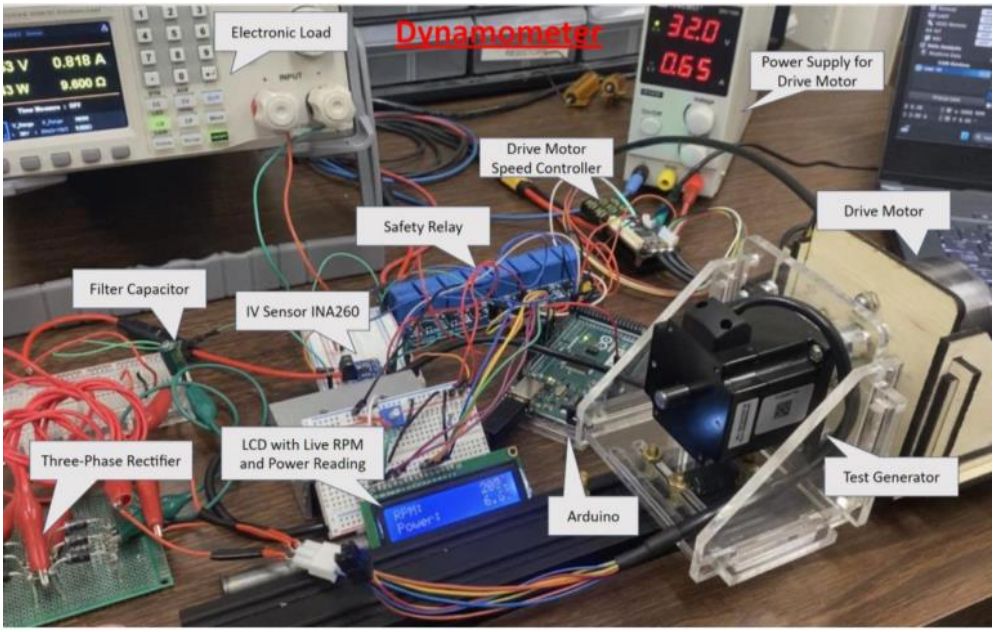

Figure 14. Dynamometer Setup

Taking inspiration from previous reports, three Lin Engineering BLDC motors were selected to serve as our generator since their specifications fell within the preliminary design expectations for our system. The preselected 24V rated generators were the BL17E40-01D (90W), the BL34E21-01D (100W), and the BL23E22-01D (60W). To determine the most efficient generator for our design, each one was tested on the dynamometer to compare their power output with respect to rpm. Each generator was tested using its calculated rated resistance. The BL17E40-01D was selected as it proved to be the most efficient with the second highest power output. Another benefit to its selection was due to its and light weight and slim design.

Figure 15. Dynamometer Test Results

Generator Selection – Performance Results From Dyno Testing

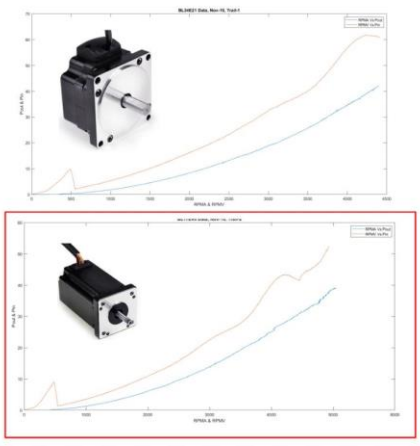

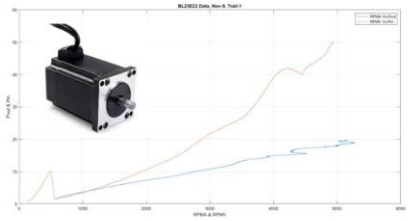

GENERATOR (BLDC Motor)	AVG. EFFICIENCY	MAX POWER OUTPUT
BL17E40-01D	57.76%	39.42 W
BL23E22-01D	57.98%	37.71 W
BL34E21-01D	45.60%	41.92 W

Developing Our Own Generator

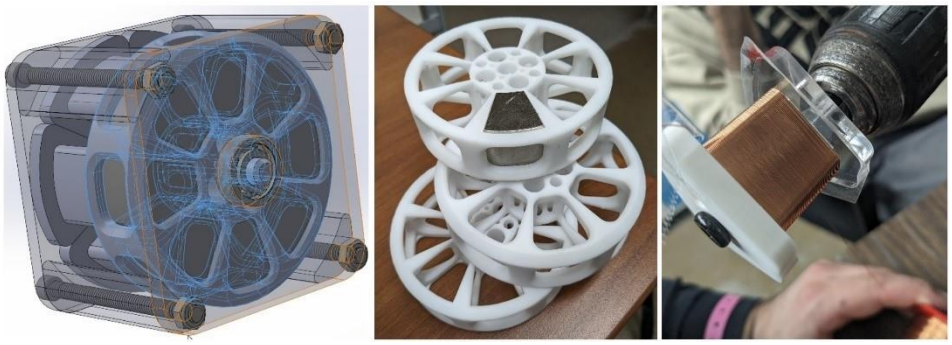

Figure 16: home build generator

As an attempt to increase power output, stability, and efficiency, we put significant effort towards developing our own permanent magnet synchronous generator (PMSG). To eliminate cogging torque, decrease cut in, and increase rpms we decided on a coreless design (eliminating the iron core in the windings). While the iron core draws the flux into the coils, we decided no cogging torque, thus improving performance at lower wind speeds, is more important than higher total power output. Similarly, we decided on a Halbach array (90 deg pole rotation with each magnet) to increase power stability and efficiency for the rotor with 8 pie magnets (96lb pull force per magnet). The optimal OD to ID ratio for the rotor was determined to be 2 and distributed windings were selected for the coil arrangement. As a new team, we are building everything from the ground up, making our generator design timeline run slightly behind submission deadlines, so we are going to incorporate our PMSG in next year's design.

TURBINE ELECTRONICS:

The turbine side of the electrical system housed our 24V boost converter, the objective of which is to produce 24V at as close to cut-in speed as possible and help stabilize the power output at higher wind speeds. To accomplish this, it contained a 900millihenry inductor, a total capacitance of 6700µF, and a Schottky diode. The boost converter was operated by a PID algorithm to precisely control its duty cycle. A 10KΩ resistor was put in parallel to the output to allow the converter to discharge safely during shutdowns while limiting losses in normal operation due to its high resistance. An LT1375 5V Buck converter was also included to supply power to the turbine devices which consist of the brakes, the linear actuator, as well as the hall effect and wind speed sensors.

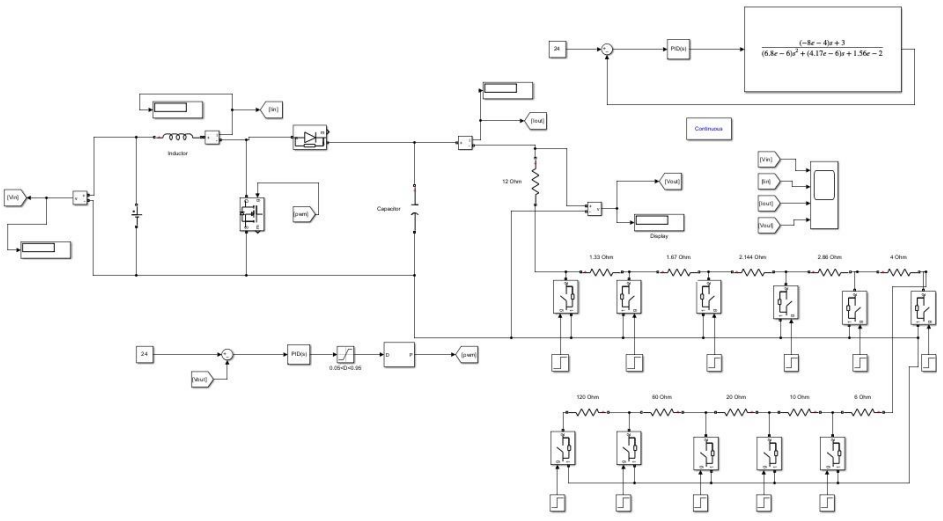

Figure 17. 24V Boost Converter Design

LOAD ELECTRONICS:

Our load electronic circuit was designed as an active current sink to ensure stable current draw by electronically controlling the drain to source resistance of four MOSFETs placed in parallel so that the current drawn by the load remains stable and changes continuously with the PCC voltage being supplied from the turbine as it spins up. A digital to analog converter takes input from the Arduino to output an analog voltage to pass through a buffer amplifier and supply the inverting inputs of the four operational amplifiers. The output of these amplifiers drive the gate pins of four MOSFETs to create an n-channel that feeds back to the amplifiers' non inverting inputs and complete the path of the PCC input voltage to ground.

To power the devices in the load, two 120/24VAC step-down transformers are used which connectto the provided 120VAC supply. The output of each of these transformers is rectified to DC using a full wave rectifier and a ripple capacitor. Linear regulators are used to provide 12V as well as ±9V to power the components within the enclosure.

Several measures were taken to ensure proper heat rejection in the load enclosure. The 4 n-channel MOSFETs were placed in parallel and outfitted with heat sinks to limit the magnitude of current through each transistor. The path through each MOSFET also terminates to its own 8Ω power resistor for additional heat dissipation. Finally, numerous vent holes and a 12V 59 CFM computer fan were installed into the enclosure to provide adequate air circulation to dissipate excess heat.

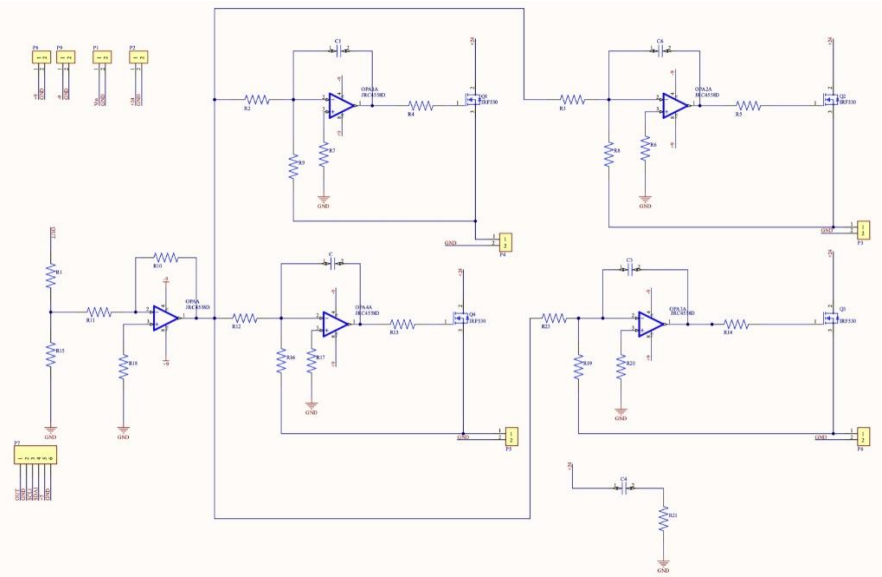

Figure 18. Electronic Load Circuit Schematic

The aim of our electronic load is to provide appropriate resistance to maintain a balanced power output from the turbine side of the electrical system. In order to know how much current to sink from the load to achieve this goal, we needed to perform different tests and simulations to calculate an expected value of load sink current. First, the selected generator for our turbine was run on the dynamometer to measure its open circuit voltage characteristics with respect to RPMs. Through wind tunnel testing of the blades, we were able to map the RPMs to each corresponding integer wind speed. This allowed us to estimate the generator's open circuit voltage with respect to wind speed. Next, QBlade simulations of our blade design allowed us to know the expected range

of incoming power from the wind. The input power of the wind was then divided by the open circuit voltage of the generator which gave us an estimation of the highest possible sink current within the load, giving us a starting point on how to program the load with respect to RPM and wind speed. Knowing this as the theoretical maximum load current allowed us to design the load to both provide adequate resistance to balance input power and withstand highest case input current allowing us to also ensure proper heat rejection.

DYNOMOMETER		WIND TUNNEL		QBLADE		LOAD CALC.
Gen. RPM	Open Ckt. Voltage	Wind Speed	RPM	Input Wind Power min (W)	Input Wind Power max (W)	Current
1000	6.9	5	968.1	2.5	3	0.36
1200	7.72	6	1246.7	4.65	5.5	0.6
1500	8.95	7	1525.3	8.15	9.65	0.91
1800	10.16	8	1803.9	12.1	14.5	1.19
2100	11.36	9	2082.5	17.5	21	1.54
2400	12.55	10	2361.1	25.5	30.5	2.03
2600	13.33	11	2639.7	33.8	40.55	2.54

Table 1: Electronic Load Current Sink Calculation

Control Model and State Diagram

The operation of our system is determined by the rpm of the turbine with the wind sensor serving as a secondary alternative. Our system's states consist of idle, power curve, control & durability, safety 1, and safety 2. Idle state is the state of our system in which cut-in wind speed has not yet been reached. Upon 5m/s wind speed, (~1000rpm) the system will transition into the power curve state in which the goal is to produce stable power output. The boost converter and electronic load work together to achieve this goal. As the windspeed increases above 11m/s (~2600rpm), the system state moves into the control & durability state in which the turbine will incorporate the pitching system to maintain the rpm and power produced by the turbine at 11m/s. As the wind speed progresses toward the maximum of 22m/s, if rpm cannot be stabilized through active pitching, the system will continuously pitch until full pitching is reached and the blades are in parked position. Our decision to combine the control and durability tasks in the same control state was due to the limitations of our wind tunnel, which is not able to produce sufficiently high wind speeds above 10m/s. Our 24V electrical system design and our pitching system's ability to fully pitch the blades gives us the confidence that our system will be able to complete the durability task effectively.

To accommodate both the emergency and push-button shut down conditions, two separate safety states are incorporated into the state machine of the wind turbine to facilitate the safe shut-down and restart of the system. The push button shutdown causes the system to enter safety state 1. When the PCC is disconnected, the Arduino will read 0V using the load side INA 229 voltage and current sensor and force the system into safety state 2. Upon entering either safety state, the Arduino sends a signal which activates the brakes and two relays on the turbine side to disconnect the generator and create a path to draw auxiliary power from the load through the PCC. A third relay on the load side is also switched to complete the path allowing the current to flow from the auxiliary power supply across the PCC to the

turbine 5V buck converter. Upon powering the 5V buck converter, the turbine devices are then energized and ready to restart the turbine at the Arduino's command once the emergency condition is cleared by either the push button restart or load reconnection. All relays are then set back to their normal operating states and the auxiliary power supply is disconnected. The brakes are then released, allowing the turbine to restart.

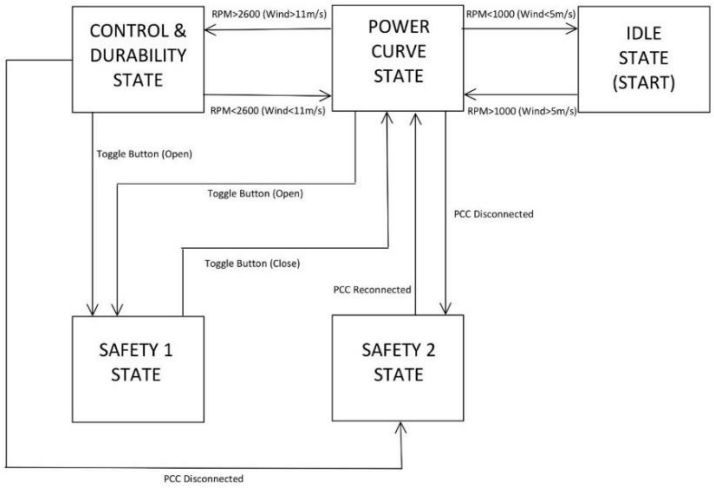

Figure 19. Control State Diagram

Physical Layout

The physical layout of our system contains two 12" x 12" x 6" NEMA electrical enlosures. One houses the turbine electronics while the other, the load electronics. Non-metallic clamp connectors facilitated wiring entrances into the enclosure ensuring adequate strain and chaff protection. Wiring between the turbine enclosure and the turbine was comprised of three cables with three Molex connectors to facilitate connection at the turbine stub to the pre-wired nacelle devices. The wiring consisted of two 18/4 cables and one 18/8 cable. The two 18/4 cables carried the power output from the generator, ground and power to the nacelle devices such as the brake, linear actuator, RPM and wind sensor. The 18/8 Cable was dedicated for the signal communication to the nacelle devices, in order to separate power and signal communication. The wiring between the enclosures included the PCC connection with Anderson power pole connectors for connection to the PCC. Communication between the load and turbine enclosures were optically isolated. Below shows the physical layout of our electrical system and our systems one-line diagram for further connection details respectively.

Figure 20. Electrical System Physical Layout

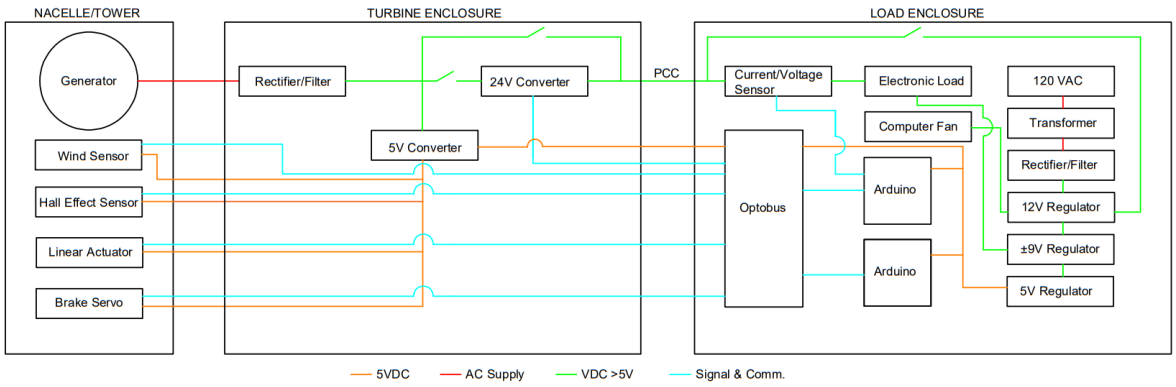

Figure21: Electrical Physical Layout

Commissioning Check List

Step	Installer initial	Verifier initial
Feed power and communication cables through foundation	SV	DB
Install foundation in the tank by inserting helical anchors	DB, SV	
Feed connections through stub and secure stub to foundation	DB, SV	DB
Verify foundation is level and place in wind tunnel	DB	SV
Connect cables between stub and tower		
Connect tower to stub, securing it with three bolts and wingnuts	DB,SV	DB
Align and secure yaw mechanism in wind direction	DB	SV
Verify blades are pitched to optimal cut in pitch	DB	AN
Verify all hardware and casings are present and secured adequately	DB	SV
Connect Cables from turbine encloser to the turbine	SV	SS
Plug in 120V AC power supply for load	SV	SS
Connect Turbine Enclosure to PCC with Anderson Pole Connectors	SV	SS
Connect Load Enclosure to PCC with Anderson Pole Connectors	SV	SS
Connect Load Enclosure to Emergency Shutdown Button	SV	SS
Ensure all electronics are powered on	SV	SS
Ensure microcontrollers communicate successfully with sensors	SV	SS
Tell judges we are ready		DB

References

M. Selig, “UIUC Airfoil Coordinates Database,” UIUC Applied Aerodynamics Group. [Online]. Available: https://m-selig.ae.illinois.edu/ads/coord_database.html#M

Ira H Abbott *et al.*, “Summary of Airfoil Data,” Jan. 1945.

Micro Linear Actuators & Servos - Actuonix Motion Devices, “L16-R Miniature Linear Servos for RC & Arduino 50mm 150:1 6 volts,” Actuonix. [Online]. Available: https://www.actuonix.com/l16-50-150-6-r

D. Wood, *Small Wind Turbines: Analysis, Design, and Application*. London: Springer.

Lin Engineering, “Brushless DC motors.” [Online]. Available: https://www.linengineering.com/products/brushless-motors/standard-bldc-motors

M. Thornton, “Lake Michigan Climatology,” LakeErieWX Marine Weather. [Online]. Available: https://www.lakeeriewx.com/CaseStudies/GreatLakesClimatology/MichiganStation45002.html

S. A. Gorji, H. G. Sahebi, M. Ektesabi and A. B. Rad, "Topologies and Control Schemes of Bidirectional DC–DC Power Converters: An Overview," in IEEE Access, vol. 7, pp. 117997-118019, 2019, doi: 10.1109/ACCESS.2019.2937239. keywords: {DC-DC power converters;Topology;Switches;Load flow;Inductors;Batteries;Batteries;bidirectional power flow;control systems;dc-dc power converters},

Tang, Y. & Lomonova, E.A. & Paulides, Johannes & Kazmin, Evgeny. (2014). Investigation of winding topologies for permanent magnet in-wheel motors.

Batzel, T.D., Skraba, A.M., & Massi, R.D. (2014). Paper 088 , ENG-xxx Design and Test of an Ironless Axial Flux Permanent Magnet Machine using Halbach Array.